Metro WDM Networks: Performance Comparison of Slotted Ring and AWG Star Networks

Hyo-Sik Yang, Martin Herzog, Martin Maier, and Martin Reisslein, *Senior Member, IEEE*

Abstract—Both wavelength-division-multiplexing (WDM) networks with a ring architecture and WDM networks with a star architecture have been extensively studied as solutions to the ever increasing amount of traffic in the metropolitan area. Studies typically focus on either the ring or the star and significant advances have been made in the protocol design and performance optimization for the WDM ring and the WDM star, respectively. However, very little is known about the relative performance comparisons of ring and star networks. In this paper, we conduct a comprehensive comparison of a state-of-the-art WDM ring network with a state-of-the-art WDM star network. In particular, we compare time-slotted WDM ring networks (both single-fiber and dual-fiber) with tunable-transmitter and fixed-receiver (TT–FR) nodes and an arrayed-waveguide grating-based single-hop star network with tunable-transmitter and tunable-receiver (TT–TR) nodes. We evaluate mean aggregate throughput, relative packet loss, and mean delay by means of simulation for Bernoulli and self-similar traffic models for unicast traffic with uniform and hot-spot traffic matrices, as well as for multicast traffic. Our results quantify the fundamental performance characteristics of ring networks versus star networks and *vice versa*, as well as their respective performance limiting bottlenecks and, thus, provide guidance for directing future research efforts.

Index Terms—Arrayed-waveguide grating, multicast, ring network, star network, throughput-delay performance, wavelength division multiplexing.

I. INTRODUCTION

TODAY'S metropolitan area networks (MANs) are mostly synchronous optical network (SONET)/synchronous digital hierarchy (SDH) ring networks which suffer from a number of drawbacks. Due to their voice-centric TDM operation and symmetric circuit provisioning bursty asymmetric data traffic is supported only very inefficiently. Furthermore, SONET/SDH equipment is quite expensive and significantly decreases the margins in the cost-sensitive metro market. This prevents new companies from entering the metro market. The inefficiencies of SONET/SDH ring networks create a severe bandwidth bottleneck at the metro level. The resultant so-called *metro gap*

prevents high-speed clients, e.g., Gigabit Ethernet, from tapping into the vast amounts of bandwidth available in the backbone [1]. In order to: 1) bridge this bandwidth abyss between high-speed clients and backbone; 2) enable new applications benefiting from the huge amounts of bandwidth available in the backbone; and 3) stimulate revenue growth, more efficient and cost-effective metro architectures and protocols are needed [2].

Wavelength-division-multiplexing (WDM) networks have been extensively investigated as solutions to the metro gap. As discussed in more detail in Section I-A, studies typically focus on either the ring [3] or the star topology [4], [5] and significant advances have been made in the medium access control (MAC) protocol design and performance optimization of the WDM ring and the WDM star, respectively. However, very little is known about the relative performance comparison of ring and star networks. In this paper, we conduct a comprehensive comparison of state-of-the-art ring and state-of-the-art star metro WDM networks. Our findings reveal the respective strengths and weaknesses of ring networks and star networks. We also identify the bottlenecks that limit the ring/star performance.

In our paper, we focus on the performance metrics throughput and delay, which are evaluated for the individual source-destination node pairs, as well as aggregated (averaged) for the entire network. We also examine the relative packet loss for the individual source-destination node pairs, as well as aggregated for the network. We note that aside from these packet level metrics, metro WDM networks could be evaluated for a number of other metrics, such as call level performance (call blocking probability) for networks that allow for a mix of packet and circuit switched traffic. Also, the capital and operational expenditures could be interesting metrics for comparison. In addition, the network survivability and protection in the face of equipment and/or fiber failures are important aspects of metro WDM networks. Both ring networks and star networks require protection which can be achieved with dual-fiber rings in ring networks and components in parallel to the star hub, as studied in [6]–[8], in star networks. Comparing the relative performance tradeoffs of these protection strategies for metro WDM ring and star networks is beyond the scope of this paper. In this to the best of our knowledge, first relative performance comparison of ring and star WDM networks, we focus on the elementary packet level metrics to get a first understanding of the relative ring and star strengths and weaknesses.

This paper is structured as follows. In the following section, we review related work. In Section II, we describe the architectures and medium access control (MAC) protocols of the considered single-fiber and dual-fiber ring networks. In Section III, we describe the architecture and MAC protocol of the considered

arrayed-waveguide grating (AWG)-based star network. In Section IV, we present our comparative simulations of ring and star WDM networks. We consider uniform and nonuniform traffic matrices for Bernoulli and self-similar traffic. We study the impact of fairness control on the performance of ring networks. We also compare the performance of ring and star networks for multicasting traffic. We summarize our findings in Section V.

A. Related Work

In this section, we give an overview of the existing literature on: 1) ring WDM networks; 2) star WDM networks; and 3) relative performance comparisons of different types of WDM networks. Ring WDM networks consist either of a single-fiber ring (as considered in most studies) or a dual-fiber ring, see for instance [9]. The nodes are equipped with either one fixed-tuned transmitter and an array of fixed-tuned receivers (FT–FR$^\Lambda$) [10], an array of fixed-tuned transmitters and one fixed-tuned receiver (FT$^\Lambda$–FR) [11], [12], or two arrays of fixed-tuned transmitters and fixed-tuned receivers (FT$^\Lambda$–FR$^\Lambda$) [13], [14], where Λ denotes the number of wavelengths in the system. Alternatively, the array of fixed-tuned transceivers can be replaced with one tunable device, e.g., a TT–FR node structure [15]. For cost and scalability reasons, it is generally desirable to deploy a small number of transceivers at each node and decouple the number of wavelengths from the number of nodes. Therefore, we consider ring networks in which each node is equipped with one single transceiver and each wavelength is shared by multiple nodes [16], [17], as described in greater detail in Section II.

Most star WDM networks for the metro area are based on the broadcast-and-select passive star coupler (PSC) [4], [5]. Star WDM networks based on the wavelength-routing AWG have recently attracted attention both for metropolitan area networks [18]–[22] and national-scale networks [23], [24]. It was shown in [25] that AWG-based single-hop networks clearly outperform their PSC-based counterparts in terms of throughput, delay, and packet loss due to spatial wavelength reuse. Therefore, in our comparison, we consider a single-hop star WDM network that is based on a wavelength-routing AWG, as outlined in Section III.

The relative performance comparison of WDM networks with different topologies has received very little attention so far. We are only aware of the delay comparison between ring and bus networks [26] and a comparison of the fiber requirements and resilience features of a multistar network and a ring network [6].

II. SLOTTED RING WDM NETWORK

A. Network Architecture

In this section, we describe the basic architecture of an all-optical WDM ring network with N nodes and Λ logical wavelength channels and a TT–FR node structure. We consider initially the single-fiber network, which connects all nodes with a single unidirectional fiber [17], and then the dual-fiber network which connects all nodes with two counterdirectional fibers [9]. In the single-fiber network, the fiber bandwidth is divided into Λ wavelength channels. Each channel is divided
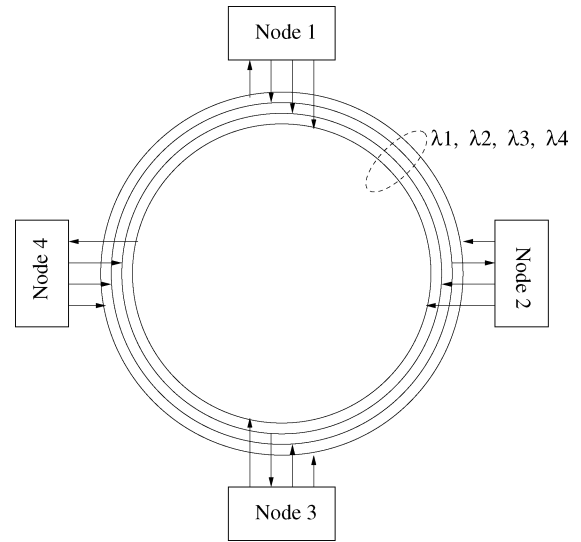

Fig. 1. Single-fiber network architecture with $N = 4$ nodes and $\Lambda = 4$ wavelength channels.
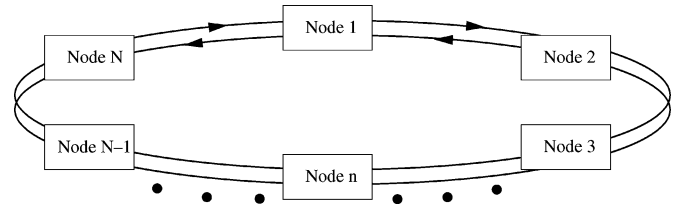

Fig. 2. Dual-fiber ring network architecture.

into fixed-length time slots whose boundaries are synchronized across all wavelengths. The slot duration equals the transmission time of a fixed-size packet. (We note that variable-size packets can be accommodated on ring networks using for instance the mechanisms studied in [9].) Each node is equipped with one tunable transmitter and one fixed-tuned receiver (TT–FR). A node can send packets on any wavelength, while it is able to receive packets only on a preassigned *drop wavelength*. For $N = \Lambda$, each node has its own separate *home channel* for reception, as shown in Fig. 1 for $N = \Lambda = 4$. For $N > \Lambda$, each wavelength is shared by several nodes for the reception of packets. Specifically, the destination nodes $j = i + n \cdot \Lambda$ with $n \in \{0, 1, \ldots, \lceil N/\Lambda \rceil - 1\}$ share the same drop wavelength i, $i \in \{1, 2, \ldots, \Lambda\}$. Consequently, nodes sharing the same drop wavelength have to forward packets toward the destination node, resulting in *multihopping*. The destination node takes the packet from the ring (destination stripping). With this destination stripping, wavelengths can be *spatially reused* by downstream nodes, leading to an increased network capacity. To avoid head-of-line (HOL) blocking each node deploys $(N - 1)$ *virtual output queues* (VOQs), one for each destination node. Each VOQ holds up to B packets.

In the dual-fiber ring network, the N nodes are interconnected with two counter-directional fiber rings, as illustrated in Fig. 2. To investigate the effect of the counterdirectionality in the fibers, we assign $\Lambda/2$ wavelength channels to each fiber, for a total of Λ channels, as in the single-fiber ring network. In a dual-fiber network, the node structure of the single-fiber network is typically duplicated, i.e., there are one TT and one FR for each fiber
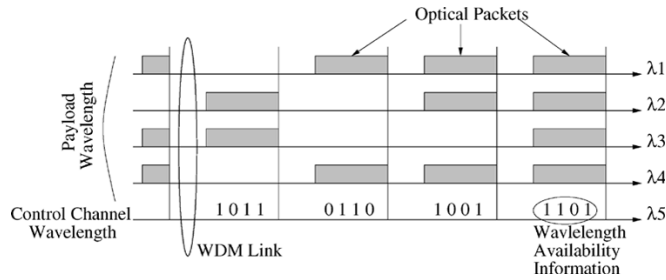
Fig. 3. Control information transport on control channel: control information in a slot corresponds to data (payload) wavelength occupancy in next slot.

[9]. The TT^2–FR^2 node structure allows a node to send and to receive two packets simultaneously. Each node has a home channel on each of the fibers.

B. MAC Protocol

In this section, we outline the MAC protocol employed in the considered ring networks. To control the access of the nodes to the slots on the wavelength channels, every slot on each wavelength is accompanied by control information. This control information indicates whether the slot is empty or occupied by a data packet (wavelength availability information). If the slot is occupied, the control information also gives the destination address of the packet occupying the slot. The control information may be transmitted on a separate control channel (as for instance, in [9], [27], and [28]) or in a subcarrier multiplexed header (as for instance, in [16] and [29]). We describe the principles of the control information transmission by discussing the control channel approach. For details on the subcarrier multiplexing approach, we refer the interested reader to the corresponding references. With the control channel approach, the control information in a given slot on the control channel corresponds to the status of the data wavelength channels in the next slot. This is illustrated for the wavelength availability information (bits) in Fig. 3. (The destination node information is not shown to avoid overcrowding this illustrative figure.) If a bit is set to one the corresponding wavelength channel is occupied in the next slot and, otherwise, it is empty.

We note that with the control channel approach there is an additional wavelength channel for control on each fiber, for a combined total of $\Lambda + 1$ wavelength channels in the single-fiber ring network and $\Lambda + 2$ wavelength channels in the dual-fiber ring network. In addition, there is a fixed-tuned transceiver (FT–FR) at each node for each fiber to transmit and monitor the control information on the control channel on each fiber.

For the packet transmission, we consider the so-called *a posteriori* access strategy, which we outline at first for the single-fiber to highlight the main points. With the *a posteriori* access strategy, a node first checks the availability status of each slot on all wavelengths by inspecting the control information and then selects the appropriate VOQ. (This *a posteriori* strategy gives generally better performance at the expense of higher complexity compared with the *a priori* access strategy [17].) The node has to wait until an empty slot arrives on one (or more) wavelength channel(s). When an arriving slot is empty on one (or more) wavelength channel(s) the node can
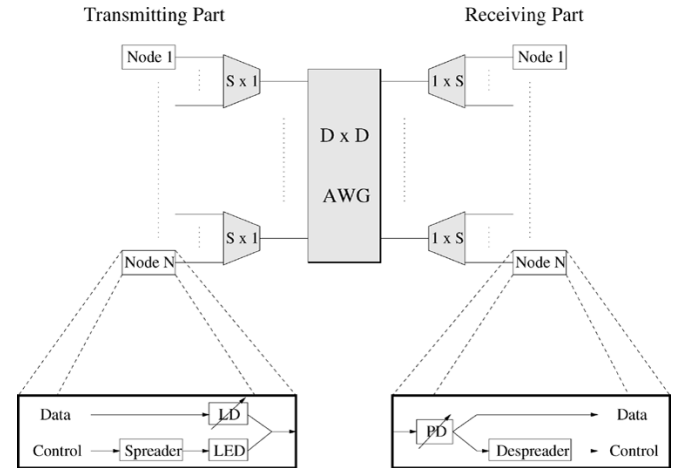

Fig. 4. Architecture of AWG-based star WDM network.

use this slot to transmit one packet from one of the corresponding VOQs. In the considered single-fiber ring architecture with per-destination VOQs, buffer selection is necessary if: 1) $N = \Lambda$ and multiple channels have an empty slot or if 2) $N \geq \Lambda$ and at least one channel has an empty slots since a node can only transmit one packet at any given time with its single transmitter. Among various buffer selection schemes, we choose the *longest queue* (LQ) selection scheme. With the LQ scheme, the longest VOQ (i.e., VOQ with the largest occupancy) is chosen. When there is a tie, the queue with the lowest index $j \in \{1, 2, \ldots, (N-1)\}$ is chosen. The motivation behind this LQ scheme is load balancing among the queues in the system, which increases the node and network throughput at acceptable system complexity [17].

In the dual-fiber ring network, the packets are transmitted in similar fashion with the *a posteriori* access strategy. The two main adaptations of the access strategy outlined for the single-fiber network to the dual-fiber network are: 1) that a node can transmit up to two packets simultaneously and 2) that a packet can be transmitted in either direction along the ring. Different strategies for choosing the direction are studied in Section IV-C.

We remark that the packet transmissions according to the wavelength availabilities require fast-tunable transmitters with a tuning time that is a small fraction of the slot duration, which is on the order of a few microseconds for typical scenarios, see Section IV-A. This requirement will be fulfilled by the recently reported fast-tunable transmitters with tuning times on the order of a few nanoseconds, see for instance [30] and [31].

III. AWG-BASED STAR WDM NETWORK

A. Network Architecture

As shown in Fig. 4, the star network is based on a $D \times D$ AWG used as a wavelength-routing device. A wavelength-insensitive $S \times 1$ combiner is attached to each AWG input port and a wavelength-insensitive $1 \times S$ splitter is attached to each AWG output port. Thus, the network connects $N = D \cdot S$ nodes. Each node is equipped with a laser diode (LD) and a photodiode (PD) for data transmission and reception, respectively. Both data transmitter and receiver are tunable over Λ wavelengths which are not preassigned to nodes (TT–TR). Similar to the ring network, each
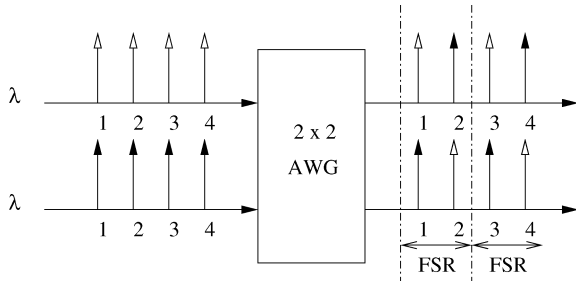
Fig. 5. Illustration of wavelength routing in AWG with $D = 2$ input and output ports when $R = 2$ FSRs are used. Each FSR provides one wavelength channel between an input–output port pair. A total of $D \cdot D \cdot R = D \cdot \Lambda = 2 \cdot 4$ wavelength channels connect the input ports to the output ports.

node has $(N - 1)$ VOQs, one for each destination. Again, each VOQ holds up to B packets. The number of available wavelengths Λ span R adjacent free spectral ranges (FSRs) of the underlying AWG, each FSR consists of D contiguous wavelength channels, i.e., $\Lambda = R \cdot D$, as illustrated in Fig. 5. Note that the AWG allows for spatial wavelength reuse. As a result, the Λ wavelengths can be simultaneously applied at each of D AWG input ports, for a total of $D \cdot \Lambda$ wavelength channels connecting the D AWG input ports with the D AWG output ports. Also, note that there are R wavelength channels connecting each AWG input-output port pair.

The MAC protocol makes use of a control channel to broadcast control information. This control channel can be implemented as an inband control channel by exploiting the spectral slicing of a broadband light source in conjunction with spectrum spreading of the control signals [21], or as an out-of-band control channel, e.g., by running a PSC in parallel to the AWG [8]. In our explanation of the basic principles of the MAC protocol in the AWG star, we focus on the out-of-band control channel; we refer the interested reader to [21] for details on the inband control channel. We only note here in brief that the capacity of the inband control channel is limited to a few megabits per second due to the physical limitations of the employed broadband light source and spectrum spreading. For the out-of-band control channel, each node can be connected via an additional fixed-tuned transceiver and fiber pair to a PSC, which is operated in parallel with the AWG. This requires more hardware than the inband signaling approach but the control channel capacity is much higher. Additionally, the PSC part of the network can be used for protection of the single point of failure of star networks, as studied in [8].

B. MAC Protocol

In the considered MAC protocol, wavelengths are assigned dynamically *on demand* such that any pair of nodes is able to communicate in one *single hop*. The applied MAC protocol is an *attempt-and-defer reservation* protocol, i.e., a data packet is sent after a successful reservation, which is conducted with a control packet. The reservation protocol avoids both channel and receiver collisions of data packets. We consider a MAC protocol with data packet aggregation. That is, a single control packet makes a reservation for all (fixed-size) data packets that are destined to a given destination node (i.e., are buffered in the

corresponding VOQ), thus forming *variable-size* data packet aggregates. The data packet aggregate is kept in the VOQ until it has been transmitted.

With out-of-band signaling, the basic time unit on the control channel is the control slot. The length of the control slot is equal to the time required to send a control packet over the out-of-band control channel. For our comparisons in this paper, we consider the following packet transmission strategy with data packet aggregation. Each node employs the LQ buffer selection scheme to determine for which VOQ to send control packets. More specifically, in each control slot, each node selects the VOQ with the largest number of unscheduled packets, forms a data packet aggregate from the packets, and prepares a corresponding control packet. The control slots for control packet transmission are not fixed assigned. Instead, the control packets are sent on a contention basis using slotted ALOHA. Specifically, a given node sends its prepared control packet with probability $1/N$ in a given control slot.

After the one-way end-to-end propagation delay (i.e., half the end-to-end round-trip time) a transmitted control packet is received and collected by every node (including the sending node). This allows each node to maintain *global knowledge* of all the other nodes' activities and a node also learns whether its own control packet collided in the control packet contention or not. All nodes periodically process the successfully received control packets by executing the same first-come-first-served and first-fit scheduling algorithm, which we adopt since scheduling in very-high-speed optical networks must have low complexity. The scheduling algorithm tries to schedule the variable-size data packet aggregates within the scheduling window of prespecified length. Note that all the nodes need to execute the scheduling algorithm on the collected control packets at the same time to ensure that all nodes compute the same transmission schedule and preserve global knowledge about the ongoing data packet aggregate transmissions.

If the control packet collided in the control packet contention, or the scheduling of the data packet within the scheduling window fails, the source node retransmits the control packet in the next control slot, provided the corresponding VOQ is still the longest VOQ. Also, note that VOQs for which a control packet is currently on its way (so it is not yet known whether it will be successful or not) are not considered in the LQ selection.

IV. PERFORMANCE COMPARISON

In this section, we conduct a detailed quantitative comparison between the state-of-the-art ring and star metro WDM networks described in the preceding two sections. In our performance comparison, we focus on the packet level performance metrics, i.e., throughput, packet delay, and packet loss, which we define in Section IV-A, in which we also describe our simulation setup.

Prior to proceeding to our detailed investigations of the packet level performance, we briefly note that the ring and star networks have specific advantages and pose specific challenges at the photonics level and for implementation. We briefly review the photonic level issues arising from transmission impairments and insertion losses, which are important considerations for the choice of network topology. In particular, in ring networks, the

TABLE I
NETWORK PARAMETERS: DEFAULT VALUES
FOR BOTH RING AND STAR NETWORK

Description	Symbol	Default Value
Network diameter	Δ	91.67 km
Number of nodes	N	64
Number of wavelengths	Λ	8
Link speed	C	2.5 Gbit/sec
Propagation speed	c	$2 \cdot 10^5$ km/sec
Packet (slot) size	L	1500 Bytes
Slot duration		4.8 μsec
VOQ size (per dest. node)	B	64 packets

TABLE II
PARAMETERS SPECIFIC TO STAR: DEFAULT VALUES

Description	Symbol	Default Value
AWG degree	D	8
Splitter/combiner degree	S	8
# of used FSRs	R	1
Control packet size		2 Byte
Control channel speed (out-of-band)		333 Mbps
control slot duration		48 nsec
Scheduling window size		200 slots

insertion losses of the wavelength multiplexers and demultiplexers (which are typically based on AWGs) used in all-optical node architectures may limit the power budget and thereby the number of nodes that can be traversed without signal regeneration [32], [33]. Furthermore, ring networks are affected by amplified spontaneous emission (ASE) noise, which may accumulate over long all-optical paths with multiple amplifiers. This accumulated ASE noise along with other impairments, such as fiber nonlinearities and crosstalk, may significantly degrade the signal quality, see for instance [34]. Techniques to mitigate these effects are under development; the ASE noise accumulation, for instance, can be reduced by employing variable optical attenuators [35]. Also, the signal regeneration at a ring node forwarding traffic to other nodes on its drop wavelength can overcome these limitations. In the single-hop star network, on the other hand, the AWG is passed only once between each pair of source and destination nodes. Thus, the insertion loss of the AWG and the transmission impairments do typically not severely restrict the scale of the network, and allow in fact for a national scale single-hop network [36], [37].

Another critical issue for the operation of packet-switched WDM networks is synchronization at the slot level. Ring networks allow for relatively simple synchronization even at extremely high data rates, see for instance [38]. In star networks, on the other hand, the slot synchronization is more challenging due to the distributed nature of the network nodes and the possibly different distances of the nodes to the hub of the star network. Techniques to achieve synchronization in PSC-based star networks have been studied extensively, see for instance [39]–[42, Sec. 7.2.1], and can be extended to the AWG-based star network in a straightforward manner.

A. Simulation Setup and Performance Metrics

By default, we consider typical metro networks interconnecting $N = 64$ nodes that are equidistant to each other on the circumference of a ring with a diameter of 91.67 km. The parameters used in both networks are summarized in Table I, those specific to the star are listed in Table II. The nodes are interconnected by a ring WDM network or a star WDM network with $\Lambda = 8$ wavelength channels. (In the dual-ring network there are four wavelength channels on each fiber plus two control wavelength channels, one on each fiber, resulting in a total of ten wavelength channels.) Each wavelength channel operates at a line rate of 2.5 Gb/s (OC48) and the propagation speed on the optical fiber link is set to $2 \cdot 10^5$ km/s. The packet

size is fixed to 1500 bytes, which is one of the dominant packet sizes in the Internet, as well as the maximum packet size [maximum transfer unit (MTU)] of Ethernet. The corresponding slot duration is 4.8 μs (1500 byte/2.5 Gb/s). For the star network, we set the size of a control packet to 2 bytes (which is sufficient to accommodate source and destination address and length of data aggregate) and the speed of the out-of-band control channel to 333 Mb/s, which is easily feasible.

Bernoulli and self-similar traffic are considered. In both cases, the average packet generation rate at each given node is σ, $0 \leq \sigma \leq 1$. More precisely, at a given node in each slot, a new packet is independently generated for each of the other $(N-1)$ nodes with probability $\sigma/(N-1)$. A newly generated packet is put in the corresponding VOQ of the destination node (or dropped if the VOQ is full). Similarly, for each of the destination VOQs, self-similar packet traffic with Hurst parameter 0.75 is generated from ON/OFF processes with Pareto distributed on-duration and geometrically distributed off-duration [43]. For both types of traffic the N nodes in the network generate on average $N \cdot \sigma$ packets per slot. In addition to the uniform traffic, where a packet generated by a given node is destined to any one of the other $(N-1)$ nodes with equal probability $1/(N-1)$, we consider nonuniform hot-spot traffic in Section IV-D.

In our performance evaluation, we consider the mean aggregate throughput, the relative packet loss, as well as the mean packet delay. The mean aggregate throughput is defined as the mean number of source node transmitters sending in the network in steady state. (Note that in the dual-fiber network a source node can transmit up to two packet simultaneously, as opposed to the star network with at most one active transmitter per source node.) We also study the mean throughput for individual source-destination node pairs, which equals the probability that the considered source node is transmitting a packet to the considered destination node in steady state. (Note that packets forwarded by intermediate nodes along the ring do not count toward the measured throughput; only the transmission of the original source node contributes to the throughput.)

The relative packet loss in the network is defined as the ratio of the total number of dropped packets and the total number of generated packets in the network. For some scenarios, we also study the relative packet loss of individual source-destination node pairs, which is the ratio of the total number of dropped packets of a given source-destination node pair and the total number of packets generated for the source-destination node pair.

We define the mean packet delay in the network as the time period elapsed from the generation of a packet to the complete reception of the packet in milliseconds in steady state.

We estimate the defined performance metrics from discrete event simulations. Each simulation was run for 10^6 slots (including a warm-up phase of 10^5 slots). For Bernoulli traffic, we obtained 95% confidence intervals on the performance metrics using the method of batch means. The 95% confidence intervals are too small to be seen in the figures.

B. Fairness Control in Ring Network

Due to the ring symmetry and the applied destination release, each node has a better-than-average access to channels leading to certain destination nodes and a worse-than-average access to channels leading to other destinations [15]. Spatial reuse may cause *starvation*, which occurs when a node is constantly being covered by up-stream ring traffic and, thus, is not able to access the ring for very long periods of time [44]. This fairness problem has received considerable attention in the literature [9], [15], [17], [45], [46].

In this comparative study, for both single-fiber and dual-fiber ring networks, we use the fairness control described in [17] which is a modified form of ATMR [46]. (We note that a modified fairness control of DQDB (Distributed Queue Dual Bus) called DQBR (Distributed Queue Bi-directional Ring) was proposed in [9] for dual-fiber ring networks. However, the DQBR scheme can not be directly employed in the considered network which uses destination stripping with spatial wavelength reuse and $N > \Lambda$.) The used fairness control represents a credit allocation scheme and provides fair channel access by means of a distributed credit mechanism and a cyclic reset scheme based on a monitoring approach. The fairness control algorithm works as follows. Initially, each node is allocated a predefined credit, referred to as *window size W*, and is set to the active state. The node status (active or inactive) for a channel is included in a so-called *busy address field* in the control information sent on the control channel. Each node decreases the window size whenever it uses a free slot to send a packet. If the node is still in the active state, i.e., if the window size is larger than zero, the node sets the busy address field to the node's address. When the window size reaches zero, the node changes its state to the inactive state, i.e., the node is not allowed to send any data using the wavelength and leaves the busy address field unchanged. Thus, all nodes in the network can see which nodes are in the active state. If a node receives a slot with busy address field set to the node itself, the node knows that all other nodes are in the inactive state. The node then immediately sends a reset message to all other nodes by setting the so-called *reset-request field* in the control information on the control channel and resets its window size to the predefined window size W. The node sends the reset message only once and waits for the reset message to circulate around the entire ring network. When the reset message is received by the node which sent the reset message, the message is stripped from the ring. When a node receives a reset-request, the node sets its status to the active state, sets the window size for the channel to the predefined window size W and forward the reset-request. This algorithm is invoked on all Λ channels at each node.

The window size W specifies the credit/quota of usable slots and determines the duration of the activity cycles. Thus, W represents the main parameter of the fairness control. Fig. 6 de-
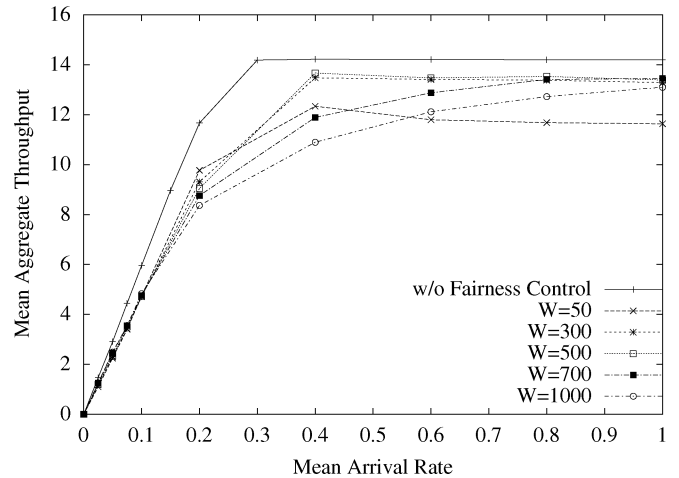

Fig. 6. Mean aggregate throughput of single-fiber ring network for uniform self-similar traffic with $W = \{50, 300, 500, 700, 1000\}$.

picts the throughput performance of the single-fiber ring network for uniform self-similar traffic without fairness control, as well as with fairness control with different window size $W = \{50, 300, 500, 700, 1000\}$. We observe and reconfirm the well-known tradeoff between (throughput) fairness and aggregate network performance, i.e., fairness control degrades the aggregate throughput performance of the network. We observe that a medium window size $W \in \{300, 500\}$ achieves the largest mean aggregate throughput. Whereas choosing a small or large W leads to a reduced throughput performance. This reduced performance is mainly due to interruptions in the transmissions caused by very frequent or infrequent consumption of the complete quota, as detailed in [47].

Unless otherwise noted, we employ for all the following simulations the ATMR fairness control with a window size of $W = 500$ in the single-fiber ring network, and a window size of $W = 1000$ in the dual-fiber ring network (which was found to give good performance for this larger window size, see [47] for details).

C. Uniform (Balanced) Traffic Scenario

We first compare the performance of the ring and star networks for uniform (balanced) traffic, where a given source node sends a generated packet to any of the remaining $(N - 1)$ nodes with equal probability $1/(N - 1)$. We consider both Bernoulli and self-similar traffic.

In the dual-fiber ring network, each packet can be sent on either of the two counter-directional rings. Two algorithms for choosing the direction are compared. With the first algorithm (Alg. 1), a packet is sent in the first empty slot that appears on either of the two rings. In the second algorithm (Alg. 2), the packet is sent on that ring which provides the smaller hop distance to the corresponding destination. We observe from Fig. 7 that with Alg. 1 the throughput improves only very slightly compared with a single-fiber ring, while Alg. 2 roughly doubles the number of concurrent transmissions at medium to high traffic loads. This is because with Alg. 2 the mean-hop distance is reduced by 50% and the spatial wavelength reuse is increased by a factor of two. We have also found that Alg. 2 gives smaller
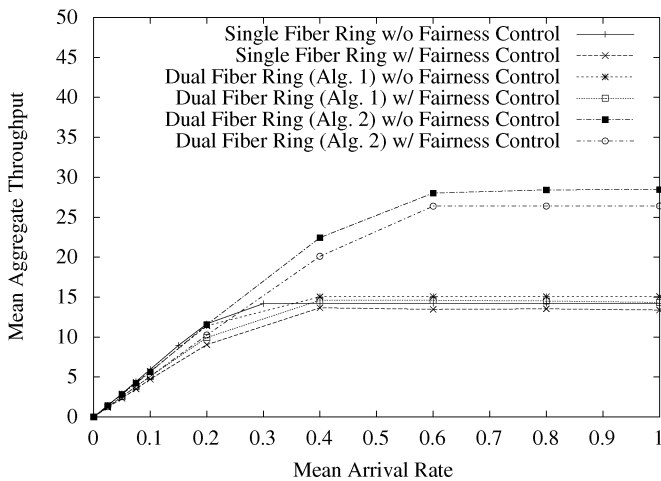
Fig. 7.   Mean aggregate throughput of ring networks for uniform self-similar traffic.
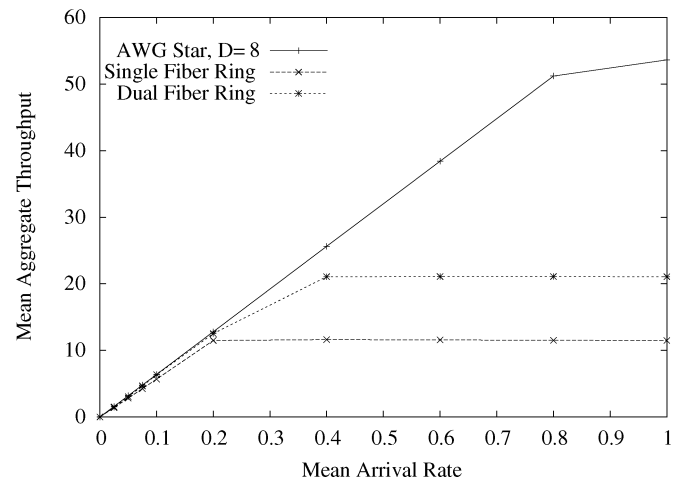

Fig. 8.   Mean aggregate throughput of star and ring networks for uniform Bernoulli traffic.
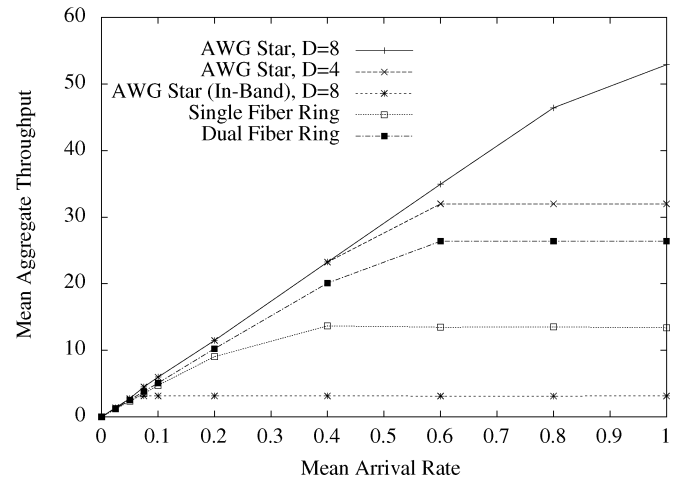

Fig. 9.   Mean aggregate throughput of star and ring networks for uniform self-similar traffic.

Fig. 10.   Relative packet loss of star and ring networks for uniform Bernoulli traffic.

delays than Alg. 1, see [47] for details. Based on these findings, we use Alg. 2 in the remainder of the paper.

Clearly, in the single-hop star network the mean hop distance is minimum (unity). The degree of spatial wavelength reuse is controlled by the AWG degree D since all Λ wavelengths can be used at each port simultaneously, as illustrated in Fig. 5. Therefore, the star network with $D = 8$, $S = 8$, and $R = 1$ is able to achieve about twice the throughput of the setup with $D = 4$, $S = 16$, and $R = 2$, which is also reflected by the results of the simulation in Fig. 9. Note that for full connectivity the maximum AWG degree is limited by $D \leq \Lambda$, resulting in an upper bound on the spatial wavelength reuse. Moreover, to fully exploit the capacity of the AWG at least $S \geq \Lambda$ nodes have to be attached to each port (cf. Figs. 4 and 5). When comparing the out-of-band signaling with the inband signaling approach (for which we consider a physically feasible speed of 3.33 Mb/s, see [47] for details), it turns out that the latter one severely limits the performance of the star network. The capacity of the inband channel does not suffice to (re)transmit all control packets leading to a much smaller throughput and to a significantly increased delay as shown in Figs. 9 and 13 (the delay with inband signaling quickly shoots up and levels out around 380 ms, which extends beyond the delay range shown in Fig. 13). In contrast, the external control channel provides sufficient capacity, leading to only few collisions and to aggregates consisting mostly of only a single packet. In the following sections, only the star with external control channel based on an AWG of degree $D = 8$ is considered.

When comparing the results of the star with those of the ring in Figs. 8–13 the latter one is clearly outperformed in terms of all measured performance metrics. The difference in the throughput of the networks, shown in Figs. 8 and 9, reflect the theoretical capacity limits of $2 \cdot \Lambda = 16$ in the single-fiber ring, $4 \cdot \Lambda = 32$ in the bidirectional ring, and $D \cdot \Lambda = 64$ in the star. In the star, up to about $\sigma = 0.8$ nearly all packets are scheduled by the first control packet leading to a small delay, depicted in Figs. 12 and 13, which is close to the theoretical minimum of two times the propagation delay of the ring diameter and nearly no packet is lost. The packet loss shown in Figs. 10 and 11 also illustrates the difference between Bernoulli and self-similar
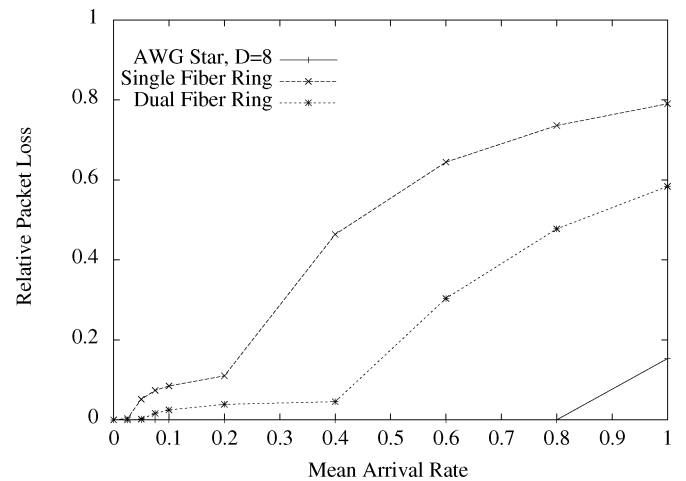
traffic. The latter one is bursty and leads to VOQ overflows even if the network is principally able to handle the offered amount of traffic and the VOQs are relatively short. As the
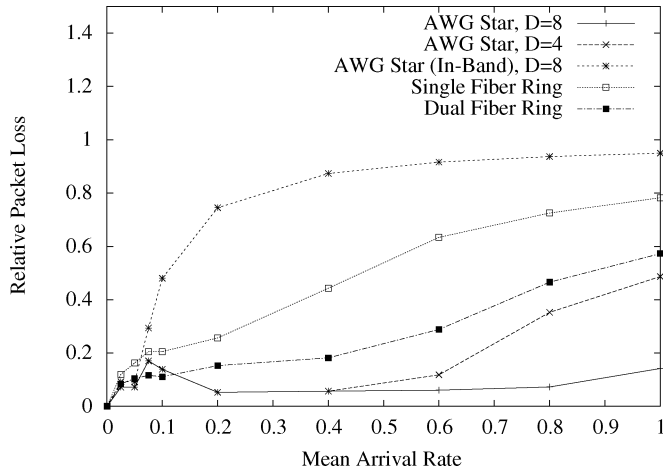
Fig. 11.   Relative packet loss of star and ring networks for uniform self-similar traffic.
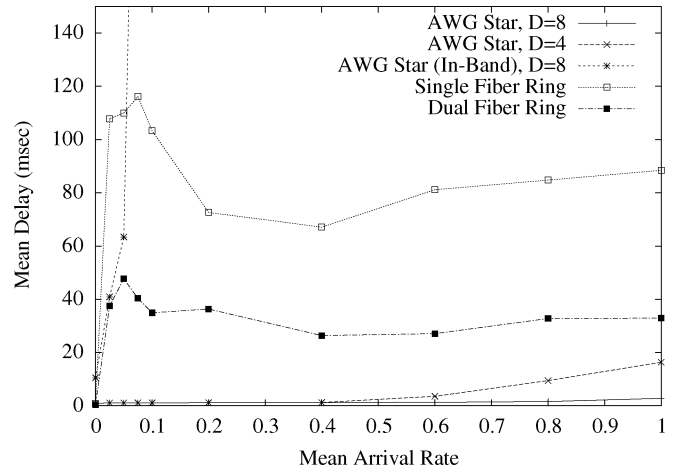

Fig. 13.   Mean delay of star and ring networks for uniform self-similar traffic.
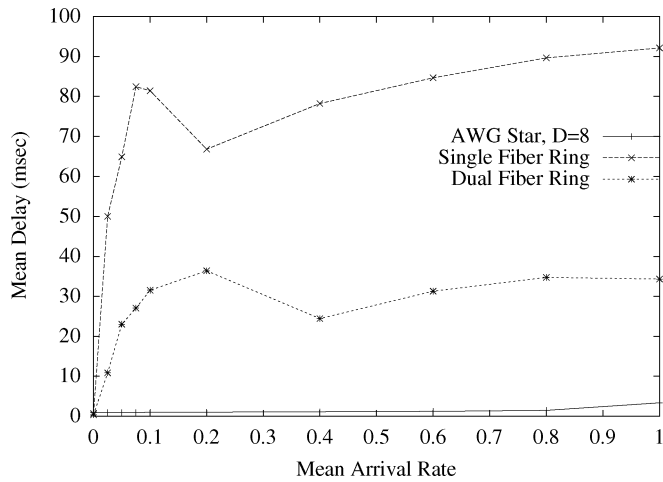

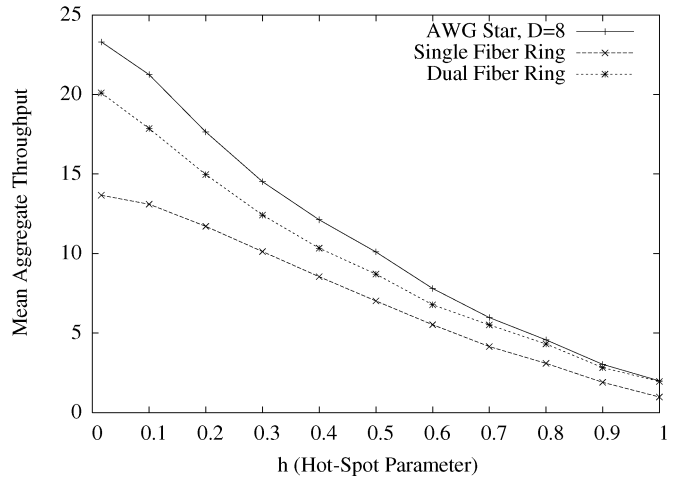Fig. 12.   Mean delay of star and ring networks for uniform Bernoulli traffic.

Fig. 14.   Mean aggregate throughput as a function of the fraction of hot-spot traffic h with $\sigma = 0.4$, fixed.

networks saturate the difference between the two traffic models vanishes. In the following, we only consider the more realistic self-similar traffic model.

D. Nonuniform (Unbalanced) Traffic Scenario

We now focus on self-similar traffic and compare the ring and star network performance for a nonuniform (unbalanced) traffic mix consisting of a uniform traffic component and a client-server traffic component. Specifically, we assume to have one hot-spot [either server or point of presence (POP)], while the remaining $(N-1)$ nodes act as identical clients. A client sends a fraction h of the traffic to the hot-spot, while the remaining fraction $(1-h)$ of the traffic is equally distributed among the other $(N-2)$ clients. Note that $h = 1/(N-1)$ corresponds to uniform traffic only as discussed above. We assume that the server generates as much traffic as all $(N-1)$ clients together and set $\sigma = 0.4$. Similar to the uniform traffic scenario, the total load offered to the network is $N \cdot \sigma$. In the ring networks, the ATMR fairness control is employed as discussed above.

The performance results are shown in Figs. 14–16. As h increases the throughput steadily decreases. For $h = 1$, the throughput of the star network is roughly equal to two, which corresponds to the one transmitter plus one receiver in the
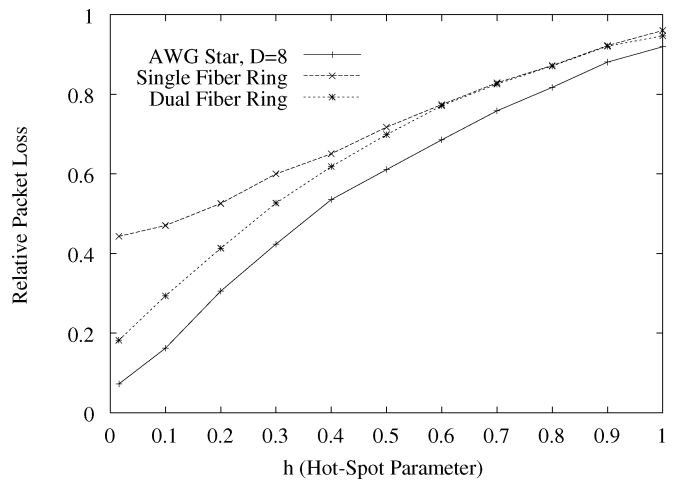

Fig. 15.   Relative packet loss as a function of the fraction of hot-spot traffic h with $\sigma = 0.4$, fixed.

hot-spot. The throughput in the ring networks for $h = 1$ is only roughly half the combined number of transmitters and receivers in the hot-spot (two in single-fiber ring network and four in dual-fiber ring network). This is due to a degeneration of the ATMR fairness control for $h = 1$, which can be overcome by
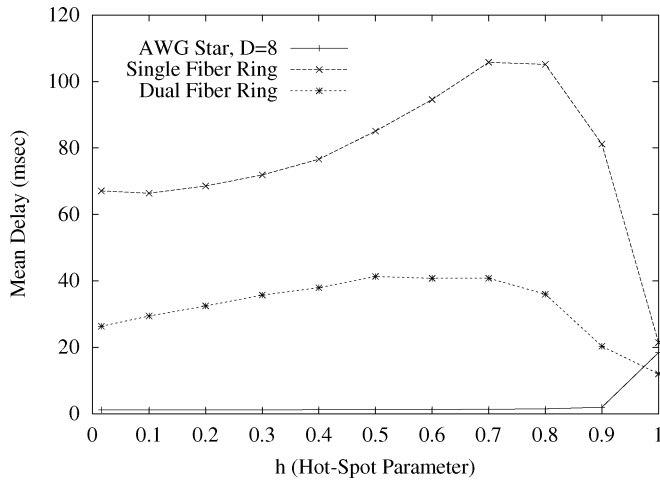
Fig. 16. Mean delay as a function of the fraction of hot-spot traffic h with $\sigma = 0.4$, fixed.
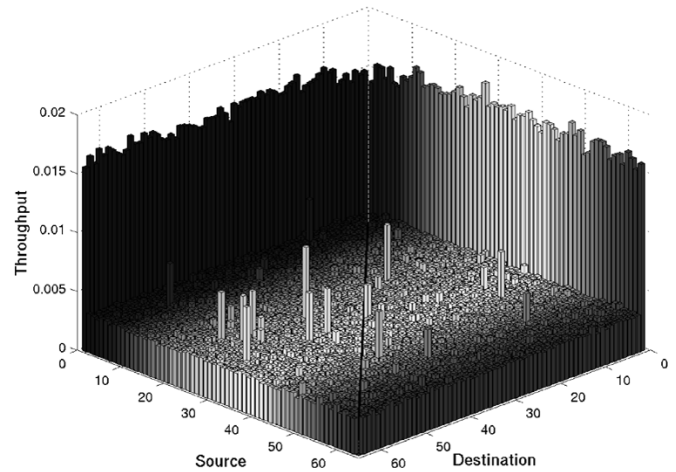

Fig. 17. Pairwise mean aggregate throughput of AWG star network for self-similar hot-spot traffic with $\sigma = 0.4$ and $h = 0.3$.

Fig. 18. Pairwise mean aggregate throughput of single-fiber ring network without fairness control for self-similar hot-spot traffic with $\sigma = 0.4$ and $h = 0.3$.

a modified fairness control, see [47] for details. Interestingly, we observe that for moderate h values in the range from approximately 0.5 to 0.8, the throughput in the single-fiber ring network is relatively close to the throughput in the dual-fiber network. We also observe that with an increasing fraction h of hotspot traffic, the relative packet loss increases steadily. This is mainly due to the limited capacity of the hot-spot's transceiver(s), which results in most of the packets destined to or originating from the server to be lost.

We observe from Fig. 16 that there are marked differences in the delay. In the star, the data aggregates corresponding to hot-spot traffic are mostly of the maximum size and experience a large delay. However, the client-to-client traffic is still transported efficiently via numerous data aggregates, mostly of the minimum size. Each received data aggregate, independent of its size, is weighted equally for the delay measurement. Therefore, the delay does not increase significantly until there is rarely any more client-to-client communication. In the ring, client-to-client traffic, except that on the hot-spot's home channel, does not experience an increased delay. In contrast, any packet transmitted on the congested home channel of the hot-spot and packets originating from the hot-spot (transmitter bottleneck) are additionally delayed. Therefore, as the fraction of hot-spot traffic increases the delay also increases. Note that for $h = 1.0$, the delay in the ring networks is smaller than in the case of uniform traffic (Fig. 13), which is due to the degeneration of the ATMR fairness control for $h = 1$, see [47] for details.

Next, we fix $h = 0.3$ and study fairness among the individual source-destination node pairs, with node 1 functioning as server. As shown in Fig. 17, the star network provides throughput fairness among all clients due to the random control packet contention and the first-come-first-served scheduling. The server achieves a larger mean throughput which is desirable since it has much more data to send than the clients. In contrast, Fig. 18 reconfirms the fairness problems in ring networks. The hot-spot, node 1, leaves most slots at its drop-wavelength empty. The succeeding nodes use these slots and achieve a high throughput to the hot-spot at the expense of the nodes further

downstream, for which no capacity is left. Only nodes downstream to the nodes which share the same drop wavelength with the hot spot, get a chance to send to the server using free slots. The source-destination pairwise metrics in the single-fiber ring network with fairness control are shown in Figs. 19 and 20. Compared with Fig. 18, the applied fairness control scheme balances the network.

E. Multicast Traffic

In this section, we compare the performance of the ring and star WDM networks for multicast (multidestination) traffic. Multicast traffic is expected to account for a significant portion of the traffic in future metro WDM networks due to applications such as video conferencing, telemedicine, distributed games, and content distribution. Multicasting in ring network has received relatively little attention [12], [48], similarly, multicasting in the AWG-based metro WDM network has received only limited attention so far [49]. In this section, we first outline the modifications to the node architectures and MAC protocols in the ring and star network to accommodate a mix of multicast and unicast traffic. We then define the considered
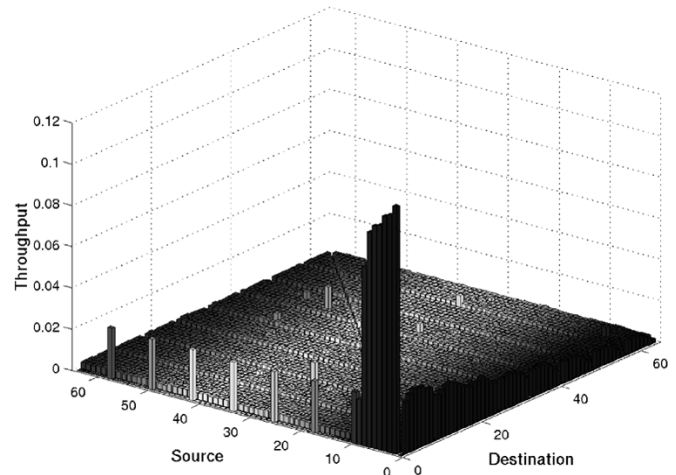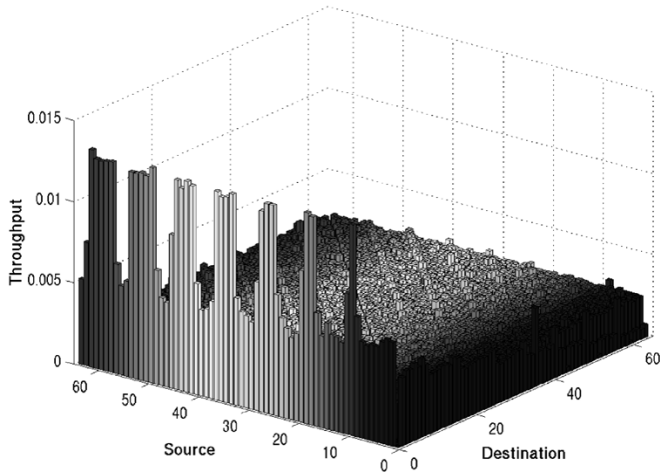
Fig. 19.   Pairwise mean aggregate throughput of single-fiber ring network with fairness control for self-similar hot-spot traffic with $\sigma = 0.4$ and $h = 0.3$.
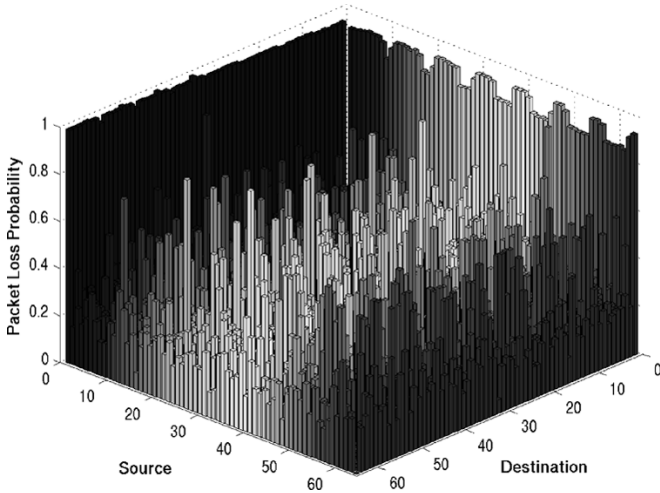

Fig. 20.   Pairwise packet loss probability of single-fiber ring network with fairness control for self-similar hot-spot traffic with $\sigma = 0.4$ and $h = 0.3$.

performance metrics for this traffic mix and present the results of our comparisons.

In both the single-fiber ring and the star network, each node is equipped with Λ buffers (each of capacity B packets) for multicast traffic (in the dual-fiber network each node has $\Lambda/2$ multicast buffers), in addition to the $N - 1$ buffers (each of capacity B packets) for unicast traffic. The multicast buffers are operated as follows. First, recall that in the single-fiber ring network each wavelength is the home channel for N/Λ nodes (in the dual-fiber ring network each wavelength on a given fiber is the home channel of $2 \cdot N/\Lambda$ nodes). Thus, a packet transmission on a given wavelength can reach up to N/Λ destination nodes of a multicast in the single-fiber ring network (or up to $2 \cdot N/\Lambda$ nodes in the dual-fiber network). Now, one of the Λ multicast buffers is assigned to each of the Λ wavelengths in the single-fiber ring network. (In the dual-fiber ring network, one multicast buffer is assigned to each of the $\Lambda/2$ home channels.) The destination nodes of a given multicast are partitioned into Λ groups in the single-fiber ring (up to $\Lambda/2$ groups in the dual-fiber ring), according to the different home channels of the destination nodes. A copy of the multicast packet is generated

for each group of destination nodes and placed in the corresponding multicast buffer. If all nodes of a given multicast share the same home channel, then only one packet copy is generated and placed in the corresponding multicast buffer. If a multicast has destination nodes on each of the home channels, then Λ packet copies are generated, and one each is placed in the Λ multicast buffers in the single-fiber network (in the dual-fiber network $\Lambda/2$ copies are generated and placed). In the star network, one of the Λ multicast buffers in a given node is assigned to each of the Λ wavelengths, or equivalently, the $\Lambda = D$ destination splitters (for the considered scenario with $R = 1$, generally, if $R \geq 1$ then R multicast buffers would be assigned to each destination splitter). The destination nodes of a multicast are partitioned according to the splitters that the destination nodes are attached to. If all destination nodes are attached to the same splitter, then one packet copy is placed in the corresponding multicast buffer. If a multicast has destinations at all splitters, then Λ packet copies are generated and one each is placed in the Λ multicast buffers.

The MAC protocol for multicast packet (copies) works as follows. The addresses of the intended destination nodes of a given multicast packet copy on a given home channel are included in the control information corresponding to the packet. Each node monitors its home channel as described in Section II-B. When a node receives a data packet, it checks whether there are additional destinations downstream. If so, the node forward the packet to the downstream nodes. If the node is the last destination, then it takes the packet off the ring. To keep the delays small for multicasts, which inherently use the bandwidth more efficiently than unicasts, we send the multicast packet copies using Alg. 1 (see Section IV-C) in the direction that has the first vacant slot.

We employ the longest queue (LQ) buffer selection in both ring and star network. We count one for a unicast packet. For a given multicast packet copy, we count the number of intended destination nodes that it will reach, i.e., up to N/Λ on the single-fiber ring and star networks, and up to $2 \cdot N/\Lambda$ on the dual-fiber ring network. This counting scheme tends to give a multicast packet copy higher priority according to the number of destination that it reaches.

In the star network, multicast packet copies are not combined into aggregates and the scheduler schedules a multicast packet copy transmission only if all intended destination nodes at the respective splitter are free.

In the performance evaluation for mixed unicast and multicast traffic, we consider the following performance metrics.

- The mean aggregate receiver throughput is defined as the number of receivers that are receiving a packet destined to them in steady state.
- The mean aggregate transmitter throughput is defined as for unicast traffic in Section IV-A.
- The mean aggregate multicast throughput is defined as the mean number of multicast completions per slot. The multicast throughput is equal to the ratio of the mean transmitter throughput to the mean number of packet copy transmissions required to reach all intended destination nodes of a given multicast packet. The multicast throughput, thus, measures the multicast efficiency of each packet copy transmission.
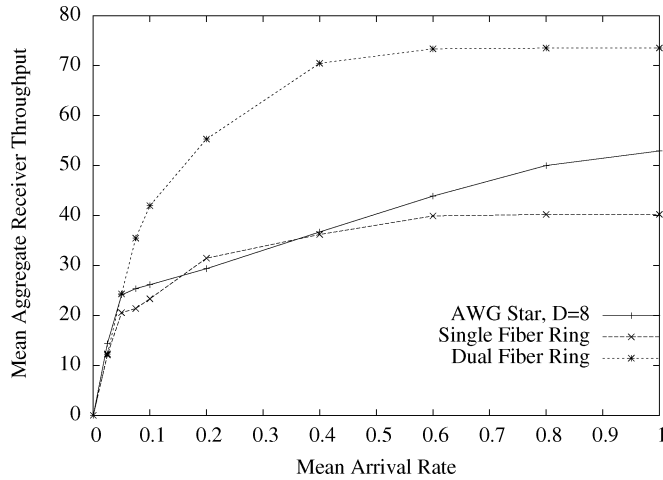
Fig. 21. Aggregate receiver throughput for uniform self-similar traffic with $p_m = 30\%$ multicast traffic.

Fig. 22. Aggregate transmitter throughput for uniform self-similar traffic with $p_m = 30\%$ multicast traffic.

- The mean packet delay is defined similar to the unicast traffic scenario in Section IV-A. For a multicast packet, however, we consider the individual delays until the complete reception of the packet by the individual receivers. The individual delays experienced until a given multicast packet is received by its destination nodes are all individually counted when evaluating the mean packet delay.
- The relative packet loss is defined as for unicast traffic, with the differences that: 1) a generated multicast packet with m destination nodes counts as m generated packets and 2) a multicast packet copy destined to n destination nodes that finds its multicast buffer full and is dropped counts as n dropped packets.

In our simulations for mixed unicast and multicast traffic, we consider uniform self-similar traffic with a fraction p_m of multicast traffic. More specifically, each node generates new packets as in the case of unicast traffic. With probability p_m a given newly generated packet becomes a multicast packet. For a given multicast packet, the number of destination nodes is drawn independently randomly from a uniform distribution over $[1, N-1]$, and the destination nodes are distributed uniformly and randomly over the other $N - 1$ nodes.

For the simulations reported here the fraction of multicast traffic is set to $p_m = 0.3$. The window size for fairness control is set as for unicast traffic to $W = 500$ in the single-fiber network and $W = 1000$ for the dual-fiber network. Figs. 21–23 give the mean aggregate receiver, transmitter, and multicast throughput as a function of the mean arrival rate σ. A number of observation are in order. First, we observe that the dual-fiber ring network achieves close to twice the receiver throughput of the single-fiber ring. This is because a packet copy transmitted on a given wavelength in the dual-fiber ring network can reach up to twice the number of nodes compared with a packet copy transmitted on the single-fiber ring. Hence, the difference in receiver throughput between single-fiber and dual-fiber ring despite both having roughly the same transmitter throughput and multicast throughput. We also observe that in both ring networks the transmitter throughput and multicast throughput have a slight peak around $\sigma = 0.2$ and then level off as the traffic load is increased further. At the same time, the receiver throughput continues to
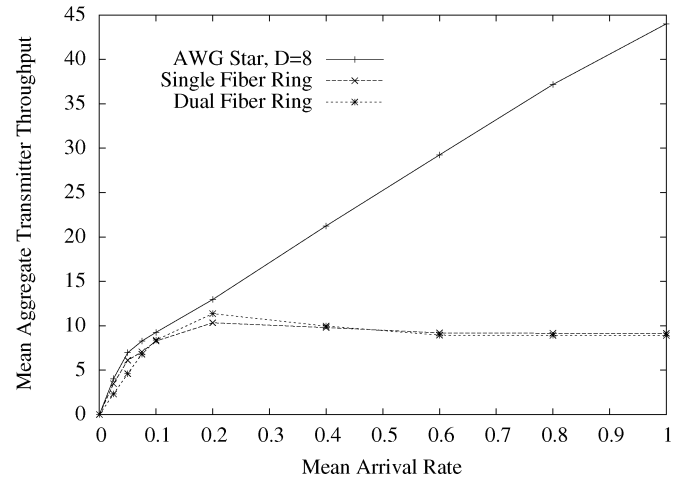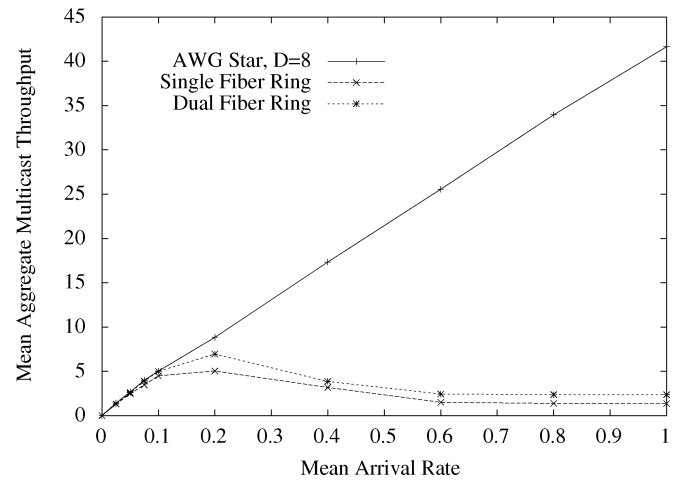

Fig. 23. Aggregate multicast throughput for uniform self-similar traffic with $p_m = 30\%$ multicast traffic.

increase. This is because the LQ buffer selection policy tends to give priority to multicast packets, especially at increasing network loads when the buffers tend to get filled (and packet loss becomes large, see Fig. 24). To see this, recall that we count the number of destination nodes of the multicast packet copies in the LQ buffer selection, as is natural and reasonable. In the single-fiber ring network, each multicast packet copy is destined on average to $N/(2 \cdot \Lambda) = 4$ destination nodes $(2 \cdot N/(2 \cdot \Lambda) = 8$ in the dual-fiber network). Thus, a unicast packet buffer completely filled with B packets has about the same priority in the buffer selection as a multicast buffer filled to a quarter of its capacity in the single-fiber network (1/8 in the dual-fiber network). As the multicast buffers are filled up to higher levels they are given priority over unicast packet buffers. More specifically, priority is given to the multicast buffer holding the packet copies with the largest number of destinations.

For the star network, on the other hand, we observe that transmitter and receiver throughput, as well as multicast throughput continue to increase as the traffic load increases. The receiver throughput, however, stays well below the levels reached by the dual-fiber ring. This is due to the combined dynamics of buffer selection and data packet scheduling in the star network. Similar
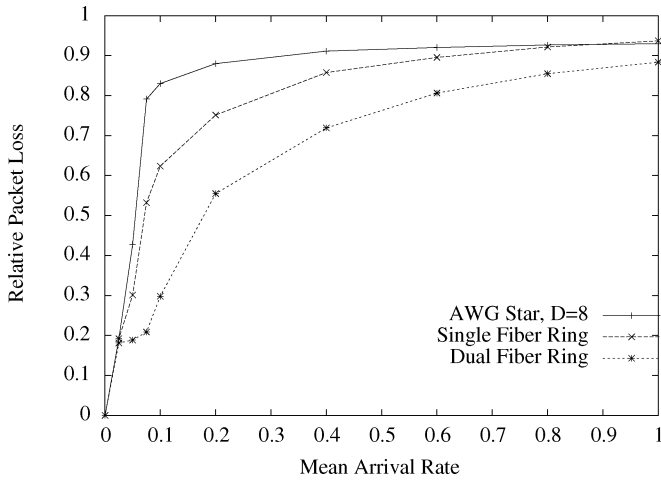
Fig. 24. Relative packet loss for uniform self-similar traffic with $p_m = 30\%$ multicast traffic.
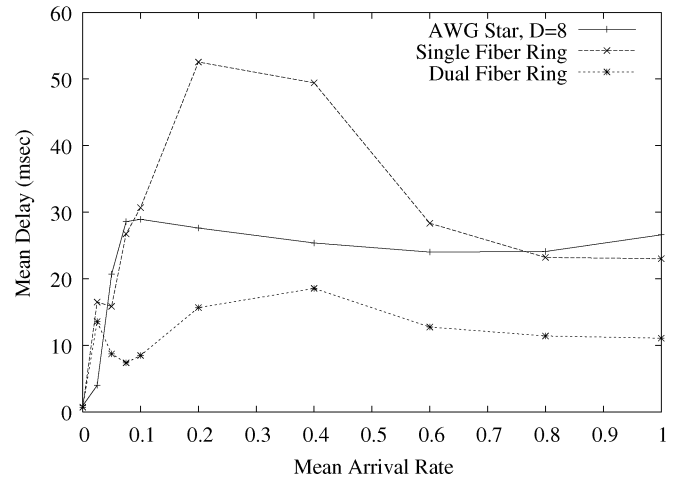

Fig. 25. Mean aggregate delay for uniform self-similar traffic with $p_m = 30\%$ multicast traffic.

to the ring network, the multicast packet copies are given priority in the LQ selection of the VOQs for which control packets are sent. The multicast data packet copies, however, are more difficult to schedule than unicast packets, as the copies require all intended receivers at a given splitter to be free in the same slot. Therefore, the scheduling of multicast packets becomes difficult, especially as the traffic load increases. As a consequence, at high traffic loads the star network tends to transmit unicast packets (and a few multicast packet copies with a small number of destination nodes). (In ongoing work, we are addressing this bias against multicast packets, one strategy is to partition the intended receivers at a splitter into subgroups.) The unicast packets are transmitted with moderate delay as they tend to experience some delay until they are selected in the buffer selection, but are then quickly scheduled. The few multicast packet copies that do eventually succeed in the scheduling, however, experience a very large delay. As a result, the average delays are significantly larger for the mix of unicast and multicast traffic in the star network (see Fig. 25) compared with the delays for unicast traffic (see Fig. 13).

In contrast, we observe that the delays for the mix of unicast and multicast traffic in the ring networks (see Fig. 25) are smaller than the corresponding delays for unicast traffic (see Fig. 13). This is because multicast packet copies (especially those with many destinations) are given priority in the buffer selection as explained above and, thus, tend to experience relatively small queue buildup and queuing delays. At the same time, multicast packets with many destinations have a large impact on the average packet delay in the network, resulting in the small delays observed in Fig. 25.

Overall, we observed from Fig. 25 that the dual-fiber ring network gives the smallest delays. The delays in the star network are roughly twice as large for a wide range of traffic loads. In the single-fiber ring network, there is a hump in the delay for moderate traffic loads (with roughly $0.2 \leq \sigma \leq 0.6$), which is due to the transmission of unicast packets that have experienced relatively large delays, see [47] for details.

Generally, we may conclude that for multicast traffic the ring networks have the advantage that there are no receiver conflicts. A multicast packet copy that is transmitted in an empty slot is delivered to all its intended destinations around the ring without requiring any coordination of the receivers. In contrast, in the TT–TR star network, destination conflicts tend to make the scheduling of multicast packet copies difficult. As we have observed in this section, the combination of these effects results in a significantly improved performance of the dual-fiber ring network over the star network. Throughout this section, we focused on the aggregate network performance for mixed unicast and multicast traffic. As we noted in the interpretations of our results, unicast and multicast traffic experience different dynamics in the considered networks with the ring networks having a bias in favor of multicast traffic and the star network having a bias in favor of unicast traffic. In ongoing work, we study the fair treatment of these traffic types.

V. CONCLUSION

We have compared the performance of state-of-the-art WDM star and WDM ring metro networks. We considered the AWG-based star network with a TT–TR node architecture, as well as the all-optical single-fiber ring with TT–FR nodes and the counter-directional dual-fiber ring with a TT^2–FT^2 node structure. In addition, fixed-tuned transceivers (FT–FR) are used in the ring networks for the transmission of control information over the control channel and for the out-of-band signaling in the AWG star network. We considered WDM ring networks with a slotted time structure and with the ATMR fairness control.

Our main finding is that the AWG star network with out-of-band signaling clearly outperforms the ring networks in terms of throughput, packet loss, and delay for unicast traffic. In addition, the star's reservation protocol naturally provides fairness and support for variable-size packets. However, the dual-fiber ring network outperforms the AWG-based star network for multicast traffic. As an architecture being relatively new to the metro area, future research should focus on solving the technological challenges of the AWG-based star network to get closer to the market. For example, fast-tunable receivers are not yet commercially available, a cost efficient external control channel is required, and cost-effective protection strategies need to be developed.

All-optical WDM ring networks, on the other hand, have proven to be technically feasible in various testbeds. The dual fiber infrastructure from existing SONET-based solutions can probably be reused for a cost-effective upgrade to the all-optical dual fiber ring, also featuring protection. Furthermore, techniques for accommodating variable-size packets in WDM ring networks are being studied, see for instance [9], and comparing them with the transport of variable-size packets in the star networks is an interesting avenue for future work. To be competitive with the star in terms of performance, future research should focus on developing new architectures allowing for a higher degree of spatial wavelength reuse.

In hot-spot traffic scenarios, both the ring and the star's performance is mostly limited by the capacity of the hot-spot's transceivers. This requires special attention in the design of the access protocol and the node structure.

ACKNOWLEDGMENT

REFERENCES

[1] P.-H. Ho and H. T. Mouftah, "A framework of scalable optical metropolitan networks for improving survivability and class of service," *IEEE Network*, vol. 16, pp. 29–35, July/Aug. 2002.

[2] B. Mukherjee, "WDM optical communication networks: Progress and challenges," *IEEE J. Select. Areas Commun.*, vol. 18, pp. 1810–1824, Oct. 2000.

[3] M. Herzog, M. Maier, and M. Reisslein, "Metropolitan area packet-switched WDM networks: A survey on ring systems," *IEEE Commun. Surveys Tutorials*, vol. 6, pp. 2–20, 2nd Quarter 2004.

[4] B. Mukherjee, "WDM-based local lightwave networks part I: Single-hop systems," *IEEE Network*, vol. 6, pp. 12–27, May 1992.

[5] M. Maier, M. Reisslein, and A. Wolisz, "Toward efficient packet switching metro WDM networks," *Opt. Networks Mag.*, vol. 3, pp. 44–62, Nov. 2002.

[6] A. M. Hill, M. Brierley, R. M. Percival, R. Wyatt, D. Pitcher, K. M. I. Pati, I. Hall, and J.-P. Laude, "Multiple-star wavelength-router network and its protection strategy," *IEEE J. Select. Areas Commun.*, vol. 16, pp. 1134–1145, Sept. 1998.

[7] Y. Sakai, K. Noguchi, R. Yoshimura, T. Sakarnoto, A. Okada, and M. Matsuoka, "Management system for full-mesh WDM AWG-star network," in *Proc. 27th Eur. Conf. Optical Communication*, vol. 3, Sept. 2001, pp. 264–265.

[8] C. Fan, M. Maier, and M. Reisslein, "The AWG‖PSC network: A performance enhanced single-hop WDM network with heterogeneous protection," in *Proc. IEEE INFOCOM*, San Francisco, CA, Mar. 2003, pp. 2279–2289.

[9] I. M. White, M. S. Rogge, K. Shrikhande, and L. G. Kazovsky, "Design of a control-based media-access-control protocol for HORNET," *J. Opt. Networking*, vol. 1, no. 12, pp. 460–473, Dec. 2002.

[10] C. S. Jelger and J. M. H. Elmirghani, "Photonic packet WDM ring networks architecture and performance," *IEEE Commun. Mag.*, vol. 40, pp. 110–115, Nov. 2002.

[11] J. Fransson, M. Johansson, M. Roughan, L. Andrew, and M. A. Summerfield, "Design of a medium access control protocol for a WDMA/TDMA photonic ring network," in *Proc. IEEE GLOBECOM*, vol. 1, Nov. 1998, pp. 307–312.

[12] R. Gaudino, A. Carena, V. Ferrero, A. Pozzi, V. D. Feo, P. Gigante, F. Neri, and P. Poggiolini, "RINGO: A WDM ring optical packet network demonstrator," in *Proc. 27th Eur. Conf. Optical Communication (ECOC 2001)*, Amsterdam, The Netherlands, Oct. 2001, pp. 620–621.

[13] J. Cai, A. Fumagalli, and I. Chlamtac, "The multitoken interarrival time (MTIT) access protocol for supporting variable size packets over WDM ring network," *IEEE J. Select. Areas Commun.*, vol. 18, pp. 2094–2104, Oct. 2000.

[14] I. Rubin and H.-K. H. Hua, "Synthesis and throughput behavior of WDM meshed-ring networks under nonuniform traffic loading," *J. Lightwave Technol.*, vol. 15, pp. 1513–1521, Aug. 1997.

[15] M. A. Marsan, A. Bianco, E. Leonardi, M. Meo, and F. Neri, "MAC protocols and fairness control in WDM multirings with tunable transmitters and fixed receivers," *J. Lightwave Technol.*, vol. 14, pp. 1230–1244, June 1996.

[16] K. V. Shrikhande, I. M. White, D.-R. Wonglumsom, S. M. Gemelos, M. S. Rogge, Y. Fukashiro, M. Avenarius, and L. G. Kazovsky, "HORNET: A packet-over-WDM multiple access metropolitan area ring network," *IEEE J. Select. Areas Commun.*, vol. 18, pp. 2004–2016, Oct. 2000.

[17] K. Bengi and H. R. van As, "Efficient QoS support in a slotted multihop WDM metro ring," *IEEE J. Select. Areas Commun.*, vol. 20, pp. 216–227, Jan. 2002.

[18] K. Kato, A. Okada, Y. Sakai, K. Noguchi, T. Sakamoto, A. Takahara, A. Kaneko, S. Suzuki, and M. Matsuoka, "10-Tbps full-mesh WDM network based on cyclic-frequency arrayed-waveguide grating router," in *Proc. ECOC*, vol. 1, Munich, Germany, Sept. 2000, pp. 105–107.

[19] A. Okada, T. Sakamoto, Y. Sakai, K. Noguchi, and M. Matsuoka, "All-optical packet routing by an out-of-band optical label and wavelength conversion in a full-mesh network based on a cyclic-frequency AWG," in *Proc. OFC 2001 Tech. Digest*, Anaheim, CA, Mar. 2001, ThG5.

[20] M. Maier, M. Reisslein, and A. Wolisz, "A hybrid MAC protocol for a metro WDM network using multiple free spectral ranges of an arrayed-waveguide grating," *Comput. Networks*, vol. 41, no. 4, pp. 407–433, Mar. 2003.

[21] M. Scheutzow, M. Maier, M. Reisslein, and A. Wolisz, "Wavelength reuse for efficient packet-switched transport in an AWG-based metro WDM network," *J. Lightwave Technol.*, vol. 21, pp. 1435–1455, June 2003.

[22] M. Maier, *Metropolitan Area WDM Networks—An AWG Based Approach*. Norwell, MA: Kluwer, 2003.

[23] N. P. Caponio, A. M. Hill, F. Neri, and R. Sabella, "Single-layer optical platform based on WDM/TDM multiple access for large-scale 'Switchless' networks," *Eur. Trans. Telecomm.*, vol. 11, no. 1, pp. 73–82, Jan./Feb. 2000.

[24] A. Bianco, E. Leonardi, M. Mellia, and F. Neri, "Network controller design for SONATA—A large-scale all-optical passive network," *IEEE J. Select. Areas Commun.*, vol. 18, pp. 2017–2028, Oct. 2000.

[25] M. Maier and A. Wolisz, "Demonstrating the potential of arrayed-waveguide grating based single-hop WDM networks," *Opt. Networks Mag.*, vol. 2, no. 5, pp. 75–85, Sept. 2001.

[26] I. Rubin and J. Ling, "Delay analysis of all-optical packet-switching ring and bus communications networks," in *Proc. IEEE GLOBECOM*, vol. 3, Nov. 2001, pp. 1585–1589.

[27] I. M. White, E. S.-T. Hu, Y.-L. Hsueh, K. V. Shrikhande, M. S. Rogge, and L. G. Kazovsky, "Demonstration and system analysis of the HORNET," *J. Lightwave Technol.*, vol. 21, pp. 2489–2498, Nov. 2003.

[28] I. M. White, M. S. Rogge, K. V. Shrikhande, and L. G. Kazovsky, "A summary of the HORNET project: A next-generation metropolitan area network," *IEEE J. Select. Areas Commun.*, vol. 21, pp. 1478–1494, Nov. 2003.

[29] K. Shrikhande, A. Srivatsa, I. M. White, M. S. Rogge, D. Wonglumsom, S. M. Gemelos, and L. G. Kazovsky, "CSMA/CA MAC protocols for IP-HORNET: An IP over WDM metropolitan area ring network," in *Proc. GLOBECOM*, vol. 2, San Francisco, CA, Nov. 2000, pp. 1303–1307.

[30] O. A. Lavrova, G. Rossi, and D. J. Blumenthal, "Rapid tunable transmitter with large number of ITU channels accessible in less than 5 ns," in *Proc. ECOC*, vol. 2, Munich, Germany, Sept. 2000, pp. 169–170.

[31] D.-R. Wonglumsom, I. M. White, K. V. Shrikhande, M. S. Rogge, S. M. Gemelos, F.-T. An, Y. Fukashiro, M. Avenarius, and L. G. Kazovsky, "Experimental demonstration of an access point for HORNET—A packet-over-WDM multiple-access MAN," *J. Lightwave Technol.*, vol. 18, pp. 1709–1717, Dec. 2000.

[32] J. J. O. Pires, M. J. O'Mahony, N. Parnis, and E. Jones, "Size limitations of a WDM ring network based on arrayed-waveguide grating OADMs," in *Proc. IFIP Int. Conf. Optical Network Design Modeling (ONDM)*, Paris, France, Feb. 1999, pp. 71–79.

[33] ——, "Scaling limitations in full-mesh WDM ring networks using arrayed-waveguide grating OADMs," *IEEE Electron. Lett.*, vol. 35, pp. 73–75, Jan. 1999.

[34] N. Antoniades, K. Ennser, V. L. da Silva, and M. Yadlowsky, "Computer simulation of a metro WDM ring network," in *Digest IEEE LEOS Summer Topical Meetings*, July 2000, pp. IV19–IV20.

[35] H. I. Saleheen, "Impact of closed cycle ASE accumulation on optical network performance," in *Proc. IEEE 14th Annu. Meeting Lasers Electro-Optics Society (LEOS)*, Nov. 2001, pp. 32–33.

[36] A. Yu, M. J. O'Mahony, and A. M. Hill, "Transmission limitation of all-optical network based on $N \times N$ multi/demultiplexer," *Electron. Lett.*, vol. 33, no. 12, pp. 1068–1069, June 1997.

[37] M. Herzog, "Design und Untersuchung von optischen metropolitan area networks (MANs) unter Berucksichtigung von neuen MAC Protokollen," Masters thesis, Inst. Photonics, Tech. Univ. Berlin, Berlin, Germany, 2002.

[38] M. A. Marsan, A. Bianco, E. Leonardi, A. Morabito, and F. Neri, "All-optical WDM multi-rings with differential QoS," *IEEE Commun. Mag.*, vol. 37, pp. 58–66, Feb. 1999.

[39] M. Cerisola, T. K. Fong, R. T. Hofmeister, L. G. Kazovsky, C.-L. Lu, P. Poggiolini, and D. J. M. Sabido IX, "CORD—A WDM optical network: Control mechanism using subcarrier multiplexing and novel synchronization solutions," in *Proc. ICC*, Seattle, WA, June 1995, pp. 261–265.

[40] I. Chlamtac, A. Fumagalli, L. G. Kazovsky, P. Melman, W. H. Nelson, P. Poggiolini, M. Cerisola, A. N. M. M. Choudhury, T. K. Fong, R. T. Hofmeister, C.-L. Lu, A. Mekkittikul, D. J. M. Sabido IX, C.-J. Suh, and E. W. M. Wong, "CORD: Contention resolution by delay lines," *IEEE J. Select. Areas Commun.*, vol. 14, pp. 1014–1029, June 1996.

[41] R. T. Hofmeister, C.-L. Lu, M.-C. Ho, P. Poggiolini, and L. G. Kazovsky, "Distributed slot synchronization (DSS): A network-wide slot synchronization technique for packet-switched optical networks," *J. Lightwave Technol.*, vol. 16, pp. 2109–2116, Dec. 1998.

[42] R. Ramaswami and K. Sivarajan, *Optical Networks: A Practical Perspective*. San Mateo, CA: Morgan Kaufmann, 2002.

[43] *Self-Similar Network Traffic and Performance Evaluation*, K. Park and W. Willinger, Eds., Wiley, New York, 2000.

[44] I. Cidon and Y. Ofek, "MetaRing – A full-duplex ring with fairness and spatial reuse," *IEEE Trans. Commun.*, vol. 41, pp. 110–120, Jan. 1993.

[45] J. Chen, I. Cidon, and Y. Ofek, "A local fairness algorithm for the metaring and its performance study," *IEEE J.Select. Areas Commun.*, vol. 11, pp. 1183–1192, Oct. 1993.

[46] K. Imai, T. Ito, H. Kasahara, and N. Morita, "ATMR: Ascronous transfer mode ring protocol," *Comput. Networks ISDN Syst.*, vol. 26, pp. 785–798, Mar. 1994.

[47] H.-S. Yang, M. Herzog, M. Maier, and M. Reisslein, "Metro WDM Networks: Performance Comparison of Ring and Star Topologies," Dept. Elec. Eng., Arizona State Univ, Tempe, AZ, Tech. Rep., [Online]. Available: http://www.fulton.asu.edu/~mre, 2004.

[48] C. Zhou and Y. Yang, "Wide-sense nonblocking multicast in a class of regular optical WDM netowrks," *IEEE Trans. Commun.*, vol. 50, pp. 126–134, Jan. 2002.

[49] M. Maier, M. Scheutzow, and M. Reisslein, "The arrayed-waveguide grating based single-hop WDM network: An architecture for efficient multicasting," *IEEE J. Select. Areas Commun.*, vol. 21, pp. 1414–1432, Nov. 2003.

Martin Herzog received the Dipl.-Ing. degree (with distinctions) in computer engineering from the Technical University of Berlin, Berlin, Germany, in 2002. He is currently working toward the Ph.D. degree with the Telecommunication Networks Group, Technical University of Berlin, where he participates in a graduate, interdisciplinary engineering research program.

His research interests lie in the area of optical wavelength-division-multiplexing (WDM) networks with a focus on architectures and access protocols for metro networks.

Martin Maier received the Dipl.-Ing. and Dr.-Ing. degrees (both with distinctions) in electrical engineering from the Technical University of Berlin, Berlin, Germany, in 1998 and 2003, respectively.

He was a Visiting Researcher at the University of Southern California (USC), Los Angeles, and Arizona State University (ASU), Tempe. Summer 2003, he spent as a Postdoctoral Fellow at the Massachusetts Institute of Technology (MIT), Cambridge. He is author of *Metropolitan Area WDM Networks-An AWG Based Approach* (Norwell, MA: Kluwer, 2003). His research interests include network and node architectures, routing and switching paradigms, protection, multicasting, and the design, performance evaluation, and optimization of medium access control (MAC) protocols for optical wavelength-division-multiplexing (WDM) networks, with particular focus on metropolitan area networks. Recently, his research interests concentrate on evolutionary WDM upgrades, control, and management of optical ring networks.

Dr. Maier was a recipient of the Two-Year Deutsche Telekom Doctoral Scholarship from June 1999 to May 2001. He is also a corecipient of the Best Paper Award presented at the SPIE Photonics East 2000-Terabit Optical Networking Conference.

Martin Reisslein (A'96–S'97–M'98–SM'03) received the Dipl.-Ing. (FH) degree in electrical engineering from the Fachhochschule Dieburg, Dieburg, Germany, in 1994, the M.S.E. degree in electrical engineering, and the Ph.D. degree in systems engineering from the University of Pennsylvania, Philadelphia, in 1996 and 1998, respectively.

He is an Assistant Professor in the Department of Electrical Engineering, Arizona State University (ASU), Tempe. During the academic year 1994–1995, he visited the University of Pennsylvania as a Fulbright Scholar. From July 1998 to October 2000, he was a Scientist with the German National Research Center for Information Technology (GMD FOKUS), Berlin, Germany. While in Berlin, he was teaching courses on performance evaluation and computer networking at the Technical University Berlin, Berlin, Germany. He maintains an extensive library of video traces for network performance evaluation, including frame size traces of MPEG-4 and H.263 encoded video, at http://trace.eas.asu.edu. His research interests are in the areas of Internet quality-of-service, video traffic characterization, wireless networking, and optical networking.

Dr. Reisslein is a corecipient of the Best Paper Award of the *SPIE Photonics East 2000—Terabit Optical Networking* Conference. He is the Editor-in-Chief of the *IEEE Communications Surveys and Tutorials* and has served on the Technical Program Committees of IEEE INFOCOM, IEEE GLOBECOM, and the IEEE International Symposium on Computer and Communications. He has organized sessions at the IEEE Computer Communications Workshop (CCW).

Hyo-Sik Yang received the B.S. degree in information and communication engineering from Myongji University, Yongin, Korea, in 1998 and the M.S. degree in electrical engineering from Arizona State University (ASU), Tempe, in 2000. He is currently working toward the Ph.D. degree in electrical engineering at ASU.

His research interests are wavelength-division-multiplexing (WDM) all-optical networks, WDM packet switching, and WDM metropolitan area networks including node architecture, optimization, medium access control (MAC) protocol, and traffic analysis and routing in mobile ad hoc networks (MANETs).